EUMETSAT Satellite Application Facility on
Support to Operational Hydrology and Water Management

Product User Manual (PUM) for product H01 new rel. (PR-OBS-1 new rel.)

Precipitation rate at ground by MW conical scanners

Reference Number: SAF/HSAF/PUM-01_new_rel.
Issue/Revision Index: 2.1
Last Change: 31 May 2013

DOCUMENT CHANGE RECORD

Issue / Revision	Date	Description
1.0	16/05/2011	Baseline version prepared for ORR1 Part 2. Obtained by PUM-01 delivered during the Development Phase.
1.1	30/09/2011	Updates, acknowledging ORR1 Part 2 review board recommendation
1.2	16/01/2012	Minor adjustments: • Document reference number as “PUM-01” instead of “PUM” • Document change record added
2.0	31/01/2013	Major changes due to release of PR-OBS-1 ver. 1.7
2.1	31/05/2013	Acknowledged updates coming from reviewers’ comments of ORR1 Part3-Delta. Title, reference, explanation changed, in order to target the document to the new version of product H01

INDEX

List of Tables

List of Figures

1 Introduction

1.1 Purpose of the document

Product User Manuals are available for each (pre)-operational H-SAF product, for open users, and also for demonstrational products, as necessary for *beta-users*.

Each PUM contains:

- Product introduction: principle of sensing, Satellites utilized, Instrument(s) description, Highlights of the algorithm, Architecture of the products generation chain, Product coverage and appearance;
- Main product operational characteristics: Horizontal resolution and sampling, Observing cycle and time sampling, Timeliness;
- Overview of the product validation activity: Validation strategy, Global statistics, Product characterisation;
- Basic information on product availability: Access modes, Description of the code, Description of the file structure.

An annex also provides general information on H-SAF.

1.2 Introduction to product PR-OBS-1

1.2.1 Principle of sensing

The new version of H01 - PR-OBS-1 product (ver. 1.7) is based on the radiometer SSMIS flown on the DMSP satellites (the former versions of PR-OBS-1 processed also SSM/I, but this sensor is no longer available, since the last SSM/I on F15 DMSP satellite is in “degraded” status). The SSMIS is now on-board the DMSP satellites F16, F17, and F18, with two additional satellites planned for 2014 (F19) and for 2020 (F20). These conical scanners provide images with constant zenith angle, that implies constant optical path in the atmosphere and homogeneous impact of the polarisation effects (see next figure).

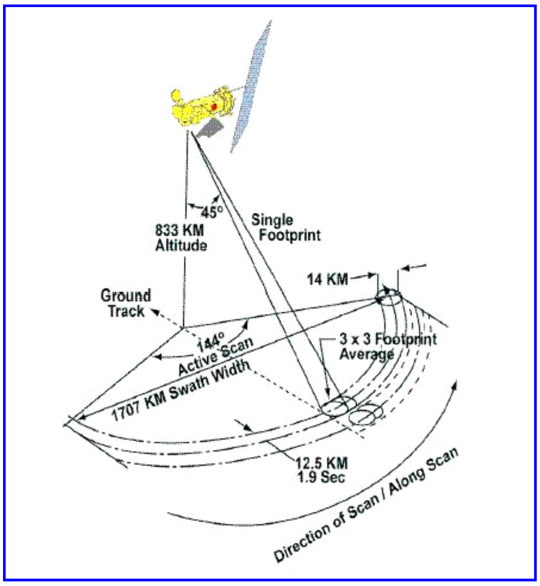

Figure 1 Geometry of conical scanning for SSMIS

Also, conical scanning provides constant resolution across the image, though changing with frequency. It is noted that the IFOV is elliptical, with major axis elongated along the viewing direction and the minor axis along-scan, approximately 3:5 of the major. Its size is dictated by the antenna diameter (actually, the antenna is slightly elliptical, to partially compensate for the panoramic distortion), but also by the portion of antenna effectively illuminated (this enables to obtain the same IFOV for a group of different frequencies, if co-registration is a strong requirement). As for the 'pixel', i.e. the area subtended as a consequence of the bi-dimensional sampling rate, the sampling distance along the satellite motion, i.e. from scan line to scan line, is invariably 12.5 km, dictated by the satellite velocity on the ground and the scan rate. Along scan, the sampling rate is selected differently for different frequencies or set of frequencies, as necessary to fulfil the radiometric accuracy requirement and to minimise aliasing.

The DMSP satellites are managed by the US Department of Defence (DoD). Raw data transmission is encrypted. Direct reception is possible by arrangement with DoD, and near-real-time acquisition could be arranged by connecting with a NATO receiving station, but currently none of the two possibilities has been implemented at CNMCA. SSMIS data are made available to Europe by NOAA. The most common access point in Europe is the UK Met Office. CNMCA acquires the data from UKMO via ftp. The delay from the end of acquisition of one orbit is in the range of 90 min.

1.2.2 Status of satellites and instruments

The current status of DMSP is shown in next table:

Satellite	Launch	End of service	Height	LST	Status	MW instruments
DMSP-F15	12 Dec 1999	expected ≥ 2010	845 km	05:40 d	Degraded	SSM/I (defective)
DMSP-F16	18 Oct 2003	expected ≥ 2013	855 km	06:25 d	Operational	SSMIS
DMSP-F17	4 Nov 2006	expected ≥ 2013	855 km	05:30 d	Operational	SSMIS
DMSP-F18	18 Oct 2009	expected ≥ 2014	857 km	08:08 d	Operational	SSMIS

Table 1 Current status of DMSP satellites (as of January 2012)

The next table collects the main features of **SSMIS**	**Special Sensor Microwave - Imager/Sounder**
Satellites	**DMSP-F16, DMSP-F17, DMSP-F18, DMSP-S19, DMSP-S20**
Status	**Operational** - Utilised in the period: 2003 to ~ 2019
Mission	Multi-purpose imagery with temperature/humidity sounding channels for improved precipitation
Instrument type	Multi-purpose imaging MW radiometer - 21 frequencies, 24 channels
Scanning technique	Conical: 53.1° zenith angle, swath 1700 km – Scan rate: 31.9 scan/min = 12.5 km/scan
Coverage/cycle	Global coverage once/day
Resolution (constant)	Changing with frequency, consistent with an antenna diameter of 61 x 66 cm
Resources	Mass: 96 kg - Power: 135 W - Data rate: 14.2 kbps

Central frequency (GHz)	Bandwidth (MHz)	Polarisations	Accuracy (NEΔT)	IFOV	Pixel
19.35	356	V, H	0.34 K	43.5 x 73.6 km	25.0 x 12.5 km
22.235	407	V	0.45 K	43.5 x 73.6 km	25.0 x 12.5 km
37.0	1580	V, H	0.24 K	43.5 x 73.6 km	25.0 x 12.5 km
50.3	380	H	0.21 K	37.7 x 38.8 km	37.5 x 12.5 km
52.8	389	H	0.20 K	37.7 x 38.8 km	37.5 x 12.5 km
53.596	380	H	0.21 K	37.7 x 38.8 km	37.5 x 12.5 km
54.4	382	H	0.20 K	37.7 x 38.8 km	37.5 x 12.5 km
55.5	391	H	0.22 K	37.7 x 38.8 km	37.5 x 12.5 km
57.29	330	RC	0.26 K	37.7 x 38.8 km	37.5 x 12.5 km
59.4	239	RC	0.25 K	37.7 x 38.8 km	37.5 x 12.5 km

60.792668 ± 0.357892 ± 0.050	106	RC	0.38 K	72.5 x 75.0 km	75.0 x 12.5 km
60.792668 ± 0.357892 ± 0.016	29.4	RC	0.37 K	72.5 x 75.0 km	75.0 x 12.5 km
60.792668 ± 0.357892 ± 0.006	10.4	RC	0.58 K	72.5 x 75.0 km	75.0 x 12.5 km
60.792668 ± 0.357892 ± 0.002	5.2	RC	0.86 K	72.5 x 75.0 km	75.0 x 12.5 km
60.792668 ± 0.357892	2.7	RC	1.18 K	72.5 x 75.0 km	75.0 x 12.5 km
63.283248 ± 0.285271	2.7	RC	1.23 K	72.5 x 75.0 km	75.0 x 12.5 km
91.655	2829	V, H	0.19 K	13.2 x 15.5 km	12.5 x 12.5 km
150	3284	H	0.53 K	13.2 x 15.5 km	12.5 x 12.5 km
183.31 ± 6.6	1025	H	0.56 K	13.2 x 15.5 km	12.5 x 12.5 km
183.31 ± 3.0	2038	H	0.39 K	13.2 x 15.5 km	12.5 x 12.5 km
183.31 ± 1.0	3052	H	0.38 K	13.2 x 15.5 km	12.5 x 12.5 km

Table 2 Main features of SSMIS

1.2.3 Highlights of the algorithm

The baseline algorithm for PR-OBS-1 processing is described in ATBD-01. Only essential elements are highlighted here.

Next figure illustrates the flow chart of the SSMIS processing chain:

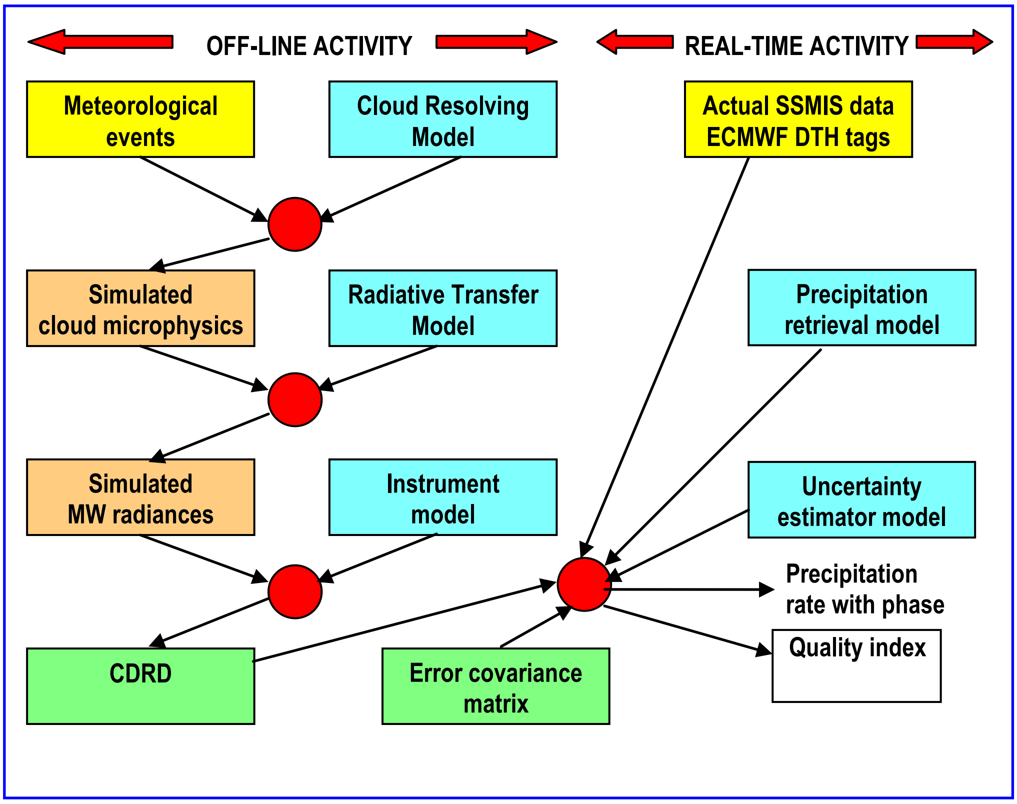

Figure 2 Flow chart of the precipitation rate processing chain from SSMIS

There is an off-line activity to prepare the Cloud Dynamic Radiation Database (CDRD) and a real-time activity to exploit the satellite data for the product retrieval. The off-line activities consist of:

- collecting well-documented meteorological events (analysis or re-analysis);
- applying a Cloud Resolving Model to simulate the cloud microphysics missing in the analysis and providing the dynamical/meteorological information to be associated to each simulated cloud microphysical structure;
- applying a Radiative Transfer Model to convert the cloud pattern in a pattern of (monochromatic) radiances at all frequencies and polarisations of the SSMIS channels;
- convoluting the monochromatic radiances with the instrument model so to simulate brightness temperatures comparable with those that would be measured from the satellite;
- finally estimate the error covariance matrix associated to the simulated T_B's in the CDRD to be used in the Bayesian retrieval algorithm.

When the satellite passes, the acquired SSMIS data are pre-processed by the instrument processor. The output of the ECMWF operational analysis and forecast system at 0.5 degrees that is closest in time of the SSMIS overpass at each location, provides the optimal dynamical/thermodynamical/hydrological constraint parameters (DTH tags) to be associated to the SSMIS observations in the retrieval process. These data are made available for the precipitation generation chain, that includes:

- an initial preparation of the dataset to be processed (sea-land mask, emissivity, selection of portion of database based on ECMWF DTH tags, …)
- the retrieval algorithm that searches for the maximum-likelihood solution in the hydrometeor profiles available in the selected portion of the CDRD, also using the error structure available in a database;
- the precipitation rate is associated to a quality index (and flag) and a phase flag.

1.2.4 Architecture of the products generation chain

The architecture of the PR-OBS-1 product generation chain is shown in the next figure:

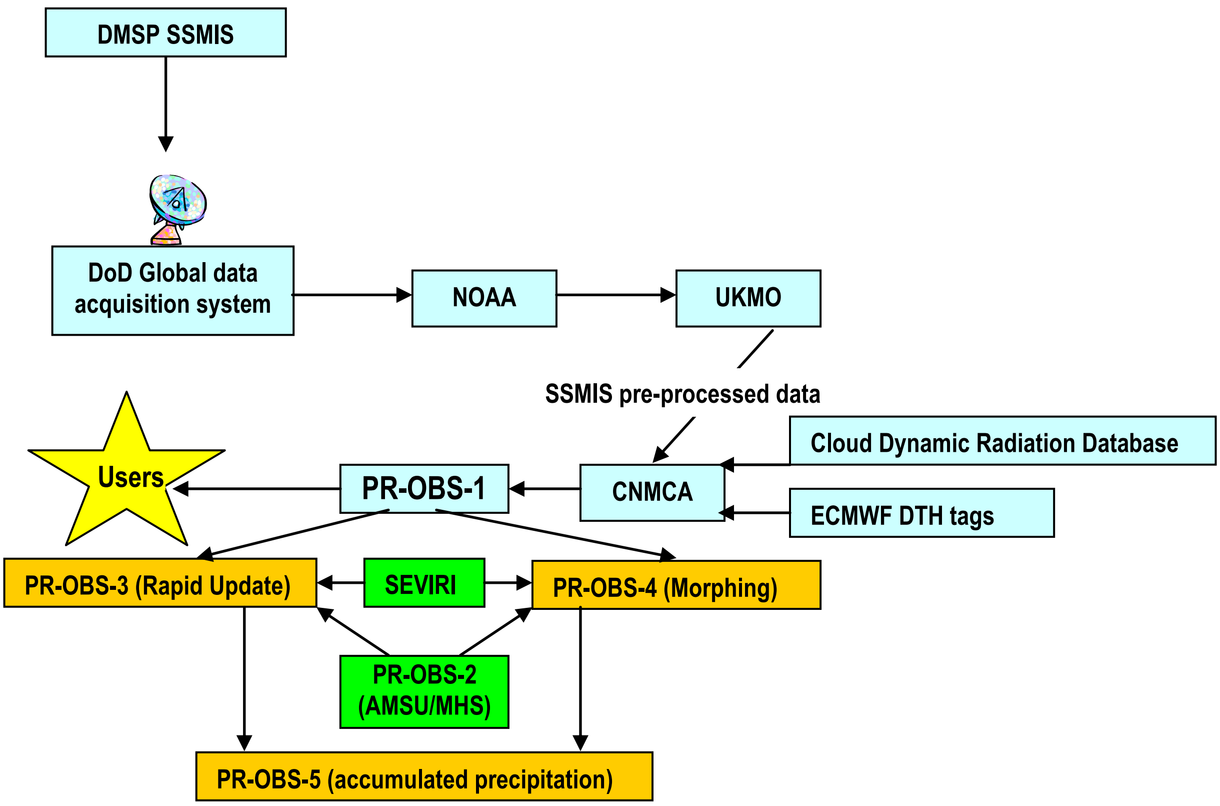

Figure 3 Architecture of the PR-OBS-1 product generation chain

A main feature of the architecture of PR-OBS-1 is the unavailability of DMSP data by direct reception or by EUMETCast. This strongly conditions the timeliness for product delivery. The data are acquired within the DoD system for global DMSP data, and conveyed to NOAA, that re-transmits them to the UK Meteorological Office (UKMO). CNMCA acquires the data from UKMO already pre-processed.

In CNMCA, the PR-OBS-1 product is generated on the base of the algorithms and the databases developed and provided by CNR-ISAC.

The product, that includes some online quality control information, is disseminated to the Users by FTP.

Figure of this section also provides information about internal utilisation of PR-OBS-1 within the overall precipitation chain in CNMCA.

One utilisation is as input to PR-OBS-3 (*Precipitation rate at ground by GEO/IR supported by LEO/MW*). In PR-OBS-3, precipitation data from PR-OBS-1 (and PR-OBS-2) are used for "calibrating" frequent SEVIRI IR-derived temperatures in terms of precipitation rate, thus generate a product at 15-min rate.

A second utilisation is as input to PR-OBS-4 (*Precipitation rate at ground by LEO/MW supported by GEO/IR, with flag for phase*). In PR-OBS-4, frequent MW-derived precipitation rate is interpolated (at 60-min intervals) from infrequent observations from LEO (PR-OBS-1 and PR-OBS-2, roughly at 3-hour intervals) by exploiting dynamic information from SEVIRI.

PR-OBS-3 and PR-OBS-4 are the base for computing PR-OBS-5 (*Accumulated precipitation at ground by blended MW and IR*).

1.2.5 Product coverage and appearance

Next figure shows the H-SAF area (25-75°N lat, 25°W-45°E lon) as covered by six successive passes of SSMIS during one day. Reading from right to left, the first three orbits are in descending phase (morning), then three are in ascending phase (afternoon). The geographic projection in this figure is *equidistant conic*. Transverse to track, the SSMIS swath is ~ 1700 km. Along track, observation is continuous as the satellite moves in orbit.

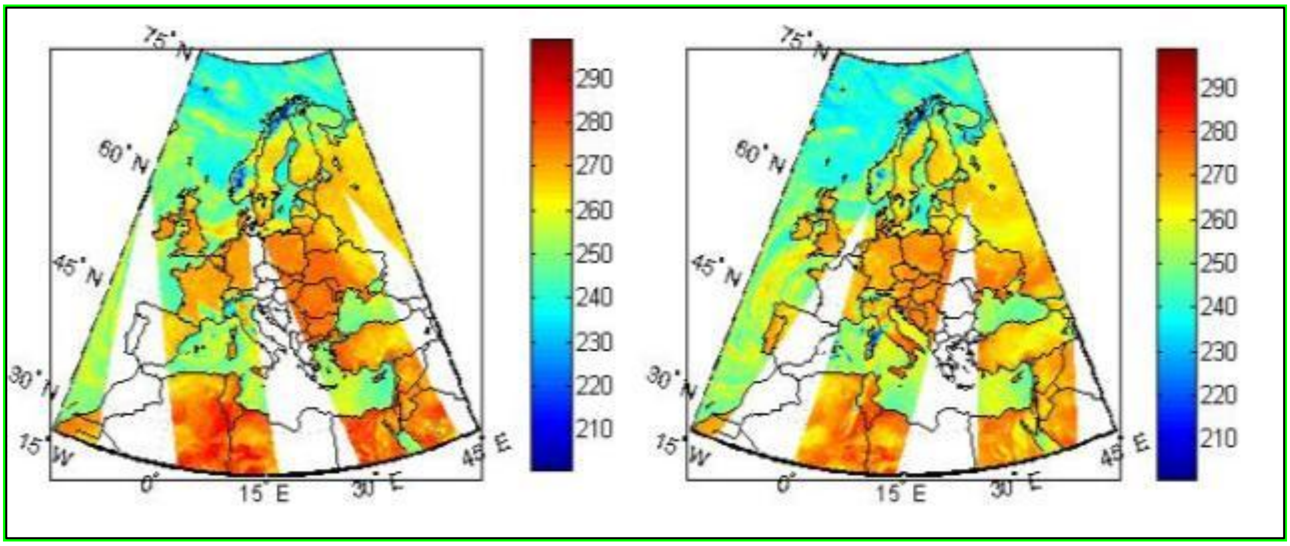

Figure 4 Coverage of the H-SAF area by an SSMIS radiometer in one day. Channel 90 GHz V. The sequence is from right to left.

Next figure show an example of precipitation product mapped in *equidistant conic projection* over a limited area of the observed field. Since data are coded as values in pixels of geographic coordinates specified in the data stream (BUFR), the product can be plotted in a projection of user's choice.

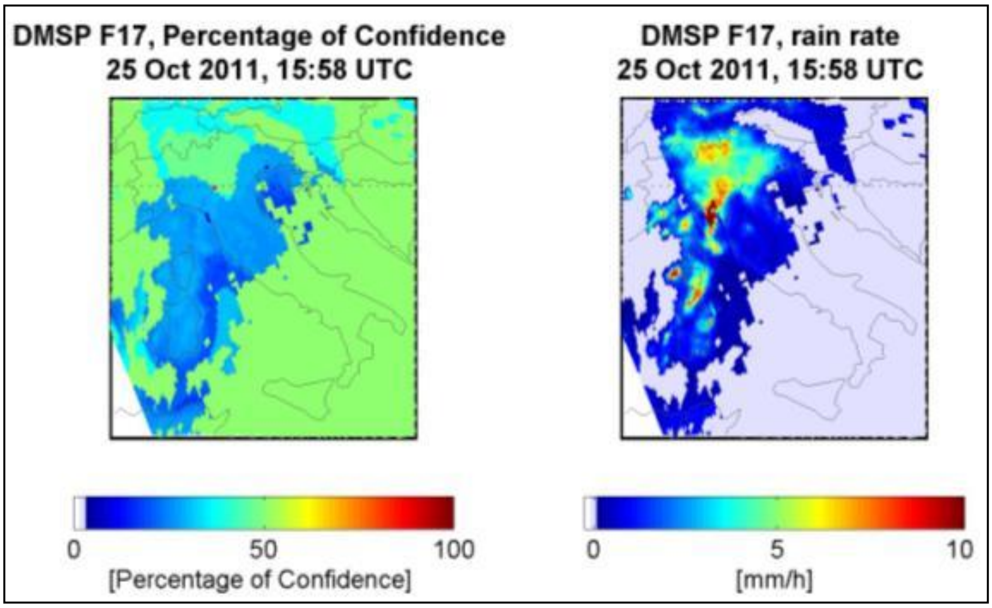

Figure 5 Example of an intensive convective event over northern Italy. The strong convective system caused the Genoa city flood during the 25th October 2010 - Left: Percentage of confidence; right retrieved precipitation [mm/h]; - Satellite DMSP-F17,SSMIS, day 25/20/2010 15:58UTC, ascending pass

Further examples follow, respectively:

- the precipitation map associated to a moderate perturbation over Hungary;
- the precipitation map associated to a snowfall event over Germany.

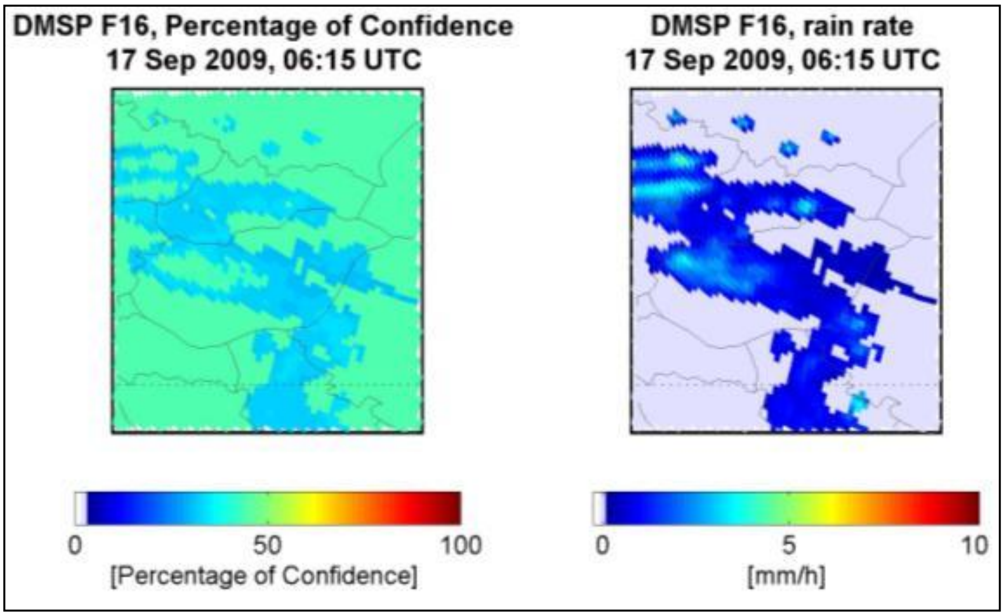

Figure 6 Example of moderate perturbation over Hungary - Left: Percentage of confidence; right retrieved precipitation [mm/h]; - Satellite DMSP-F16, SSMIS, day 19/09/2009 06:15 UTC, ascending pass.

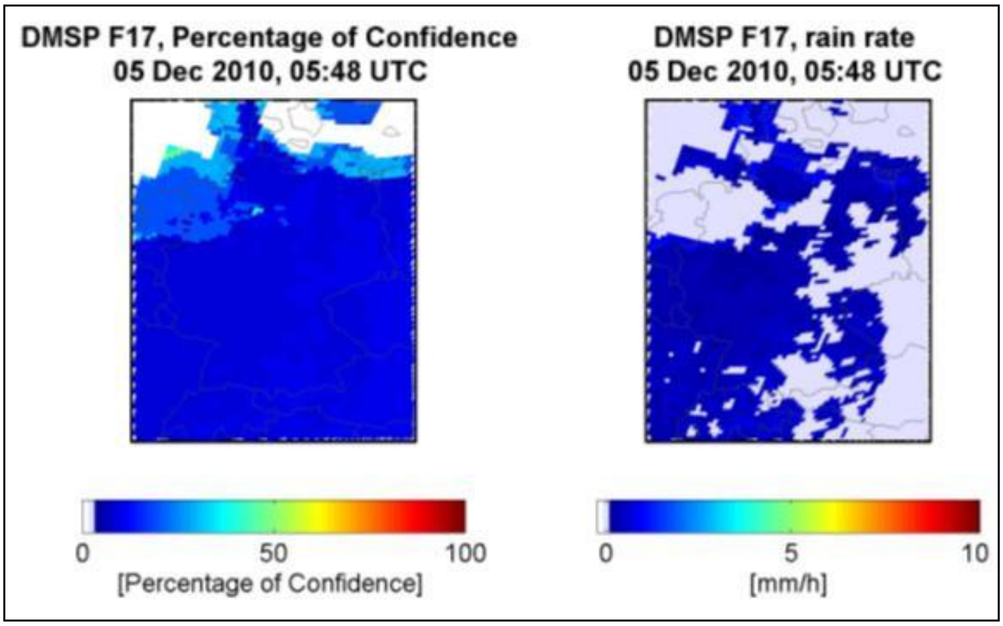

Figure 7 Example of snowfall over Germany - Left: Percentage of confidence; right retrieved precipitation [mm/h]; - Satellite DMSP-F17, SSMIS, day 05/12/2010 05:48 UTC, descending pass

The new version of PR-OBS-1 (ver. 1.7) provides also a quality index, a percentage of confidence and a phase of precipitation associated to the retrieved precipitation. Figures above show the percentage of confidence associated to the correspondent overpasses. In next figure an example is shown of the phase of precipitation for a case study over Italy (10/02/2012). For details on how the quality index and the phase flag are derived please refer to the ATBD document.

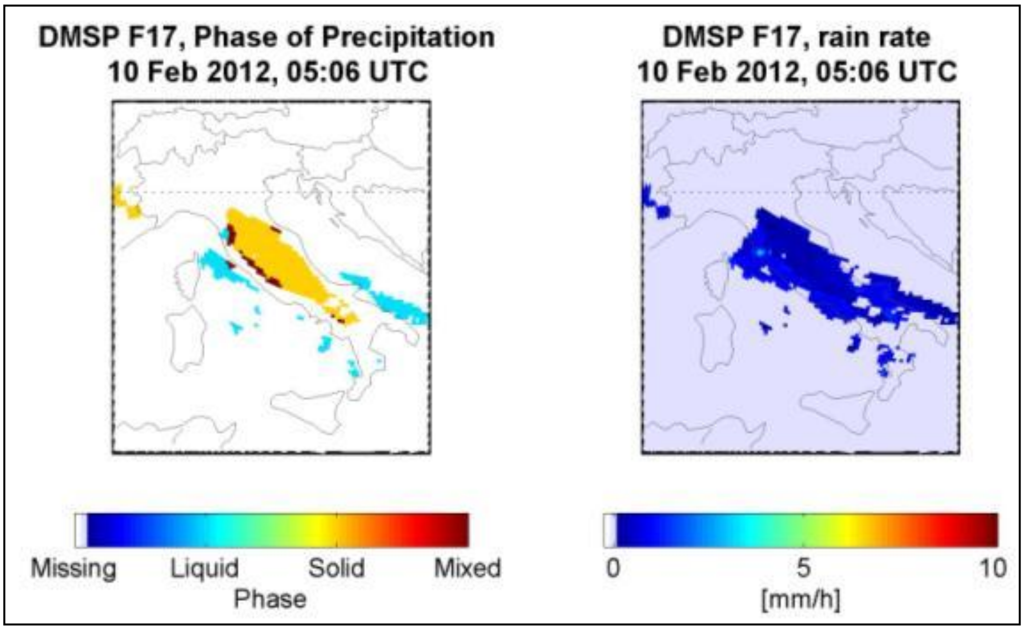

Figure 8 Phase of precipitation example Left: Phase of precipitation; right retrieved precipitation [mm/h]; - Satellite DMSP-F17,SSMIS, day 10/02/2012 05:06 UTC

1.3 Comparison between H01 (PR-OBS-1) and H02 (PR-OBS-2)

One of the main objectives of upgrading PR-OBS-1 (and PR-OBS-2) version was to be able to achieve consistency of precipitation retrievals, both in terms of precipitation pattern and in terms of quantitative estimates, from close in time cross-track scanning and conically scanning radiometer overpasses of the

same event. This achievement is crucial in order to be able to use all available overpasses for hydrological application, as well as for ingestion of all passive microwave products in the generation of other H-SAF products (i.e., PR-OBS-3, PR-OBS-4) where IR measurements form geostationary satellites are used to enhance the spatial and time resolution of the passive microwave precipitation fields. Within this framework a huge effort has been made in a new training of the PR-OBS-2 neural network by using the same cloud-radiation PR-OBS-1 database. At the same time the PR-OBS-1 screening algorithm of non-precipitating pixels has been changed and calibrated to the PR-OBS-2 screening algorithm. Finally in both algorithms new functions for the background surface and event type identification has been introduced.
Since both H01 (PR-OBS-1 ver. 1.7) and H02 (PR-OBS-2 ver. 2.4) algorithms have been developed using the same physical basis, mainly differing in their choice of solution solvers (averaging over *a priori* Bayesian probabilities for PR-OBS-1 versus neural network training based relationships for PR-OBS-2), the degree of consistency in their precipitation retrievals when the algorithms has been verified for close-in-time measurements acquired by conical and cross-track scanning radiometers for the same rainfall event.

The results of this process are provided on the product validation activity report for product PR-OBS-1 ver. 1.7:

- PVR-01: Product Validation Report for PR-OBS-1 ver. 1.7.

Figure 9 shows a comparison of retrieved surface rain rates for the two algorithms, based on DMSP/SSMIS and METOP-A/AMSU-A/MHS overpasses during the 20 October 2011 flash flood event in Rome, Italy, noting the METOP-A overpass only lags the DMSP overpass by 11 minutes. The intercomparison reveals close correspondence in rain rates for the flood event, noting that the AMSU-A/MHS scan is not centered on the main precipitation event, instead viewing the scene at the outer left scan edge where spatial resolution undergoes its greatest deterioration. There are differences between the two sets of retrievals in various light precipitation areas in eastern Europe, and although this cannot be proven, these differences may well be related to the 11-minute time difference between overpasses which would likely have its greatest effect on the lighter rain rates. Overall, even given the 11-minute time difference in overpasses and the deteriorated resolution in the cross-track scanner measurements, the intercomparison results effectively corroborate the capabilities of the two algorithms in reporting highly similar rainfall results from very different retrieval solution methodologies using greatly different radiometer scanning technologies.

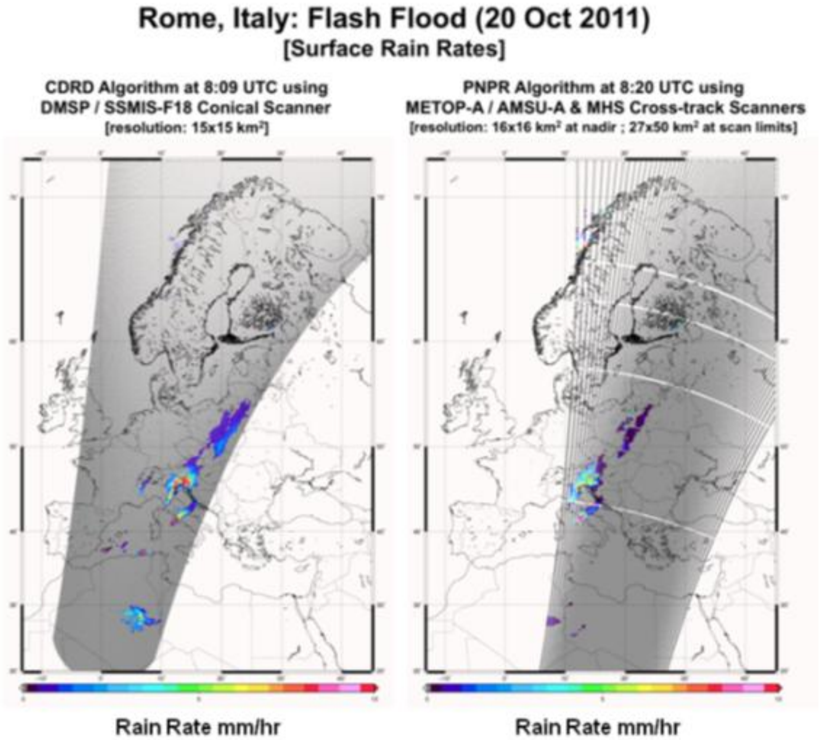

Figure 9 Comparison of retrieved surface rain rates for 20 October 2011 flash flood event in Rome, Italy

In figure above: Left panel shows results for PR-OBS-1 applied to measurements from DMSP/SSMIS-F18 conical scanner while right panel shows results for PR-OBS-2 algorithm applied to measurements from METOP-A/AMSU-A & MHS cross-track scanners. Note lag of 11 minutes between DMSP and METOP-A satellite overpasses and difference in spatial resolutions due to difference in intrinsic instrument scanning designs.

2 Product operational characteristics

2.1 Horizontal resolution and sampling

The horizontal resolution (Δx). The IFOV of SSM/I-SSMIS images changes with frequency from ~ 15 km at 90 GHz to ~ 55 km at 19 GHz). We consider the 90 GHz channel IFOV 13.2 x 15.5 km, as effective for most precipitation types. Sampling is performed at ~ 12.5 km intervals. Thus:

- resolution Δx 13.2 x 15.5 km - sampling distance: 12.5 km.

2.1.1 Vertical resolution if applicable

Not applicable.

2.1.2 Observing cycle and time sampling

The *observing cycle (Δt)* is defined as the average time interval between two measurements over the same area. In general the area is, for GEO, the disk visible from the satellite, for LEO, the Globe. In the case of H-SAF we refer to the European area shown in Fig. 04. In the case of LEO, the observing cycle depends on the instrument swath and the number of satellites carrying the addressed instrument.

As shown in Table 1, currently there are up 4 DMSP satellites in orbit, but only F16, F16, and F18 are currently operational, carrying SSMIS. Because of the limited instrument swath, the coverage is equivalent to that one of two with wide swath, that would provide global coverage at 6-hour intervals. However, the orbits crowd in the early-morning / late afternoon LST, thus the cycle is not regular, ranging from 2 to 10 hours

It is important to note that PR-OBS-2 from NOAA and MetOp provide precipitation observations at times complementary to DMSP. The sequence of LST at the equator is shown in next table:

<table>
<tr><th>Satellite (seven)</th><th>LST</th><th>Aggregation of satellites (number reduces to 4)</th><th>LST of the 4 aggregated satellites</th><th>Δ LST PR-OBS-1 + PR-OBS-2</th><th>Δ LST PR-OBS-1</th><th>Δ LST PR-OBS-2</th></tr>
<tr><td>DMSP-F16</td><td>19:10 d</td><td rowspan="2">Equivalent to one satellite
(overlapping orbits, narrow swath)</td><td rowspan="2">~ 19:30</td><td rowspan="2"></td><td></td><td rowspan="2"></td></tr>
<tr><td>DMSP-F18</td><td>19:55 d</td><td rowspan="6">10 hours</td></tr>
<tr><td>MetOp-A</td><td>21:30 d</td><td></td><td>~ 21:30</td><td rowspan="2">4.5 hours</td><td rowspan="2">4.5 hours</td></tr>
<tr><td>NOAA-18</td><td>01:45 a</td><td rowspan="2">Equivalent to one satellite
(overlapping orbits)</td><td rowspan="2">~ 02:00</td></tr>
<tr><td>NOAA-19</td><td>01:50 a</td><td rowspan="3">3.5 hours</td><td rowspan="5">7.5 hours</td></tr>
<tr><td>DMSP-F17</td><td>05:30 d</td><td></td><td>~ 05:30</td></tr>
<tr><td>DMSP-F16</td><td>07:10 d</td><td rowspan="2">Equivalent to one satellite
(overlapping orbits, narrow swath)</td><td rowspan="2">~ 07:30</td></tr>
<tr><td>DMSP-F18</td><td>07:55 d</td><td rowspan="2">2.0 hours</td><td rowspan="7">10 hours</td></tr>
<tr><td rowspan="2">MetOp-A</td><td rowspan="2">09:30 d</td><td rowspan="2"></td><td rowspan="2">~ 09:30</td></tr>
<tr><td rowspan="2">4.5 hours</td><td rowspan="2">4.5 hours</td></tr>
<tr><td>NOAA-18</td><td>13:45 a</td><td rowspan="2">Equivalent to one satellite
(overlapping orbits)</td><td rowspan="2">~ 14:00</td></tr>
<tr><td>NOAA-19</td><td>13:50 a</td><td rowspan="3">3.5 hours</td><td rowspan="5">7.5 hours</td></tr>
<tr><td>DMSP-F17</td><td>17:30 d</td><td></td><td>~ 17:30</td></tr>
<tr><td>DMSP-F16</td><td>19:10 d</td><td rowspan="2">Equivalent to one satellite
(overlapping orbits, narrow swath)</td><td rowspan="2">~ 19:30</td></tr>
<tr><td>DMSP-F18</td><td>19:55 d</td><td rowspan="2">2.0 hours</td><td rowspan="2"></td></tr>
<tr><td>MetOp-A</td><td>21:30 d</td><td></td><td>~ 21:30</td></tr>
</table>

Table 3 Sequence of equatorial crossing times of satellites providing PR-OBS-1 and PR-OBS-2

According to Table 3, the observing cycle of PR-OBS-1 as stand-alone product is, in average, ***Δt ~ 6 h***, with very irregular distribution since sampling ranges ***from 2 to 10 hours***. PR-OBS-2 also has average ***Δt ~ 6 h***, but the distribution is more regular, since sampling ranges from ***4.5 to 7.5 hours***. Most importantly, the average observing cycle of PR-OBS-1 + PR-OBS-2 is ***Δt ~ 3 h***, with sampling ranging from ***2 to 4.5 hours***.

Because of the east-west movement of a satellite in sun-synchronous orbits, the LST over Europe is ~ 1 h earlier than at the equator for ascending orbits, ~ 1 h later for descending orbits; see, for instance, Figure 4. DMSP passes over Europe occur in the intervals 5:30 to 9:30 and 15:30 to 19:30 LST.

2.1.3 Timeliness

The *timeliness (δ)* is defined as the time between observation taking and product available at the user site assuming a defined dissemination mean. The timeliness depends on the satellite transmission facilities, the availability of acquisition stations, the processing time required to generate the product and the reference dissemination means. In the case of H-SAF the future dissemination tool is EUMETCast, but currently we refer to the availability on the FTP site.

The delay between observation time and data collection at NOAA is variable with the number (unknown) of DMSP receiving stations utilised. Let's assume half orbital period (50 min). Then 90 min have to be added for availability in Rome via NOAA and UKMO. After adding ~ 10 min for processing, we have: ***δ ~ 2.5 h***.

3 Product validation

3.1 Validation strategy

Whereas the previous operational characteristics have been evaluated on the base of system considerations (number of satellites, their orbits, access to the satellite) and instrument features (IFOV, swath, MTF and others), the evaluation of accuracy requires validation, i.e. comparison with the ground truth or with something assumed as "true". The new version of PR-OBS-1 (ver. 1.7) has been validated on case studies provided by 6 Institute members of the Precipitation Products Validation Group (all except for Turkey) (see figure below).

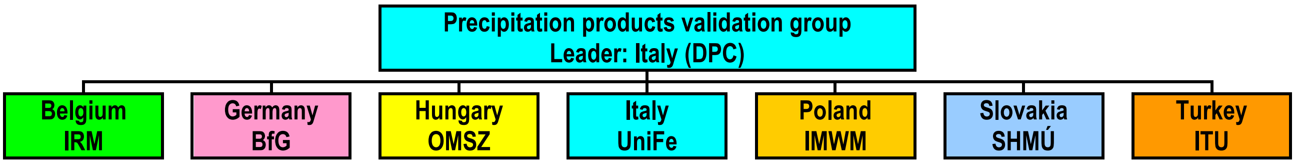

Figure 10 Structure of the Precipitation products validation team

The case studies have been selected mainly with the goal of covering a variety of precipitation events in Europe, characterized by different environmental (surface background, temperature and moisture profiles), seasonal, meteorological, dynamical conditions, and with different precipitation regimes. The reason for choosing a case study approach as opposed to a general statistics approach was due to the need of understanding in detail specific conditions where the precipitation estimate is more or less accurate, and to determine how the PR-OBS-1 (and PR-OBS-2) product quality vary in relation to the observed characteristics of each specific event. These characteristics are both related to the ground truth data used for the validation (which vary significantly among different countries in Europe, or within the same country), and to the environmental/meteorological conditions of the observed event, as well as to the sensor characteristics. The results of such validation have been very useful in defining the quality index, by identifying regions and conditions where the retrieval is more or less accurate and reliable, and in refining the precipitation screening and phase flag modules of the algorithms. Moreover, the validation has been used to assess the consistency of the PR-OBS-1 and PR-OBS-2 products for close in time overpasses of cross-track and conically scanning radiometers for the same event, a very important goal for being able to use all available overpasses in blending or morphing techniques using IR observations, and for hydrological applications.

Precipitation data have been compared with rain gauges and meteorological radar for the case studies listed in the Table below.

Before undertaking comparison, ground data and satellite data have been submitted to scaling and filtering procedures. Detailed report of the product validation activity for product PR-OBS-1 ver. 1.7 is provided as document:

- PVR-01: Product Validation Report for PR-OBS-1 ver. 1.7.

In this PUM-01 only a summary of the main results is provided, mainly aiming at characterising the product quality under different geographical/climatological conditions (those in the countries of the participating validation Units) of the different case studies.

Case study code	Date	Region	Description
IT1	20/10/2011	Italy	Rome Flood
IT2	25/10/2011	Italy	Flood over Lunigiana region
IT3	4/11/2011	Italy	Genoa flood
IT4	03-04/02/2012	Italy	Snowfall
IT5	10-11/02/2012	Italy	Snowfall
IT6	21-22/12/2009	Italy	Snowfall
HU1	10/9/2010	Hungary	Convective Event
HU2	23/6/2011	Hungary	Convective Event
HU3	30/7/2011	Hungary	Convective Event
HU4	1/12/2009	Hungary	Stratiform Event
HU5	17/9/2009	Hungary	Stratiform Event
HU6	10/2/2009	Hungary	Snowfall
PO1	11/5/2009	Poland	Convective Event
PO2	23/6/2009	Poland	Convective Event
SK1	7/6/2011	Slovakia	Orographic Precipitation
SK2	23/12/2009	Slovakia	Melting snow on frozen soil
BE1	13/11/2010	Belgium	Stratiform Event
GE1	7/8/2010	Germany	Convective Event
GE2	3/6/2010	Germany	Convective Event
GE3	05-06/12/2010	Germany	Frontal winter Event

Table 4 - Short description of the case studies

3.2 Summary of results

As a result of the validation based on case studies different problems have been highlighted concerning the ground truth data. First, there are serious differences between the different national networks data and sometimes even between different networks from the same nation (i.e. radar and rain gauges in the same area may present important biases). As a consequence it was impossible for the developers to succeed with a coherent calibration of the satellite data using the provided dataset based on case studies. In order to calibrate the satellite products it is necessary to define a high quality and well calibrated subset of ground data.
The discrepancies found between the PR-OBS-01 product and the ground truth data depends on the kind of event; this is reasonable because one of the most important source of error comes from the discrepancies in the spatial location of rain fields due to different geometry of observation (in case of radar data) or to local versus areal measurements, and the spatial distribution of the precipitation field is strongly related to the kind of event. In case of snowfall and iced precipitation the magnitude of the errors may become too high. This is due to different factors, some of which are related to issues of the satellite based algorithm in interpreting the complex radiometric signature produced by iced precipitating particles or by snow covered or frozen surface background. However, in case of snowfall (at least for not heated rain gauges) there are

very important issues also in the ground data, the discrepancies between the radar and rain gauge are so large in some case that very likely one of the two (or maybe both) is not suitable for validation purposes. A strong recommendation to the validation team coming from this study is that it is critical to threat separately the snowfall events from other kind of events in an operational and continuous statistics.

The new version of PR-OBS-1 (v.1.7) produces estimates of the phase of precipitation; the phase product needs a separate validation that was not performed in this study because this information was not provided by the ground data. The status of the background surface (including snow or frozen soil) and the phase of precipitation together with the precipitation regime (deep convective, convective, stratiform and light stratiform), the Bayesian internal variance and a satellite number (in order to take into account hardware problems of specific platforms) contribute to define a pixel based percentage confidence index and a quality flag in the new version of the two algorithms. This information needs to be always considered along with the surface precipitation rate estimates, since it can be used as a guidance to the users for a correct evaluation the reliability of the estimates, and of the results of the product validation (considering for example that a PCI equals to 0 or quality flag equals to "Missing" corresponds to data seriously corrupted that should not be included in the validation).

Considering the results of the case study analysis and the comparison of the two versions of the algorithms, the new PR-OBS-01 version (1.7) solves some serious issues of the old version, such as the miss-interpretation of the radiometric signature in presence of snow covered surfaces as strong precipitating area, or presence of large areas of false alarm in cold environmental conditions. However, a bias with ground based data is often present even if the magnitude and sign of the bias may vary from one national network to another and from radar to rain gauges. Using the Fractional Standard Error percentage (FSE%) (also referred to as the Root Mean Squared Error Percentage *to the mean "true" value*), and the RMSE, it has been shown that the PR-OBS-01 version 1.7 has usually smaller deviations from ground truth data. Both the ME and the SD are usually reduced in the new version and the correlation coefficient is higher. Finally the CSI is almost always higher, mostly due to a reduction of the FAR. The analysis of the error dependence on the rain rate magnitude has shown (in all case studies considered but one) better or equivalent performances of the new version with respect to version 1.4 currently operational, with an RMSE (and FSE%) increasing (decreasing) with the rain rate threshold considered.

	PR-OBS-01		PR-OBS-02	
	v1.4	v1.7	V2.3	V2.4
NUM	9409	8849	9710	9676
ME	0.15	-0.08	-1.03	-0.59
SD	2.56	2.37	2.68	2.22
RMSE	2.55	2.37	1.99	1.97
FSE%	174.19	161.84	123.32	121.78
CC	0.36	0.39	0.51	0.50
POD	0.70	0.70	0.68	0.68
FAR	0.61	0.52	0.50	0.48
CSI	0.33	0.40	0.41	0.42

Table 5 Comparison between H01 and H02: summary table

In table 5 the summary of error statistics for both old and new versions of PR-OBS-1 and PR-OBS-2 are compared. The statistics is based on all available and reliable ground data, from all types of events considered, and from both the analysis against radar and rain gauges data together. In order to do so we have considered only rain gauge data over Italy, both radar and rain gauges over Germany, and radar over Hungary, Poland and Slovakia. Case studies with snowfall were not considered for this table. It is evident the improvement between the old (v1.4 for PR-OBS-01 and v2.3 for PR-OBS-2) and the new (v1.7 for PR-OBS-01 and v2.4 for PR-OBS-2) versions of both the algorithms. This is confirmed by the low values of ME, SD, RMSE and FSE% and by the reduction of the FAR respect to the same POD value (and the consequent lower value of CSI).

A huge effort has been made in the development of two new versions of products PR-OBS-01 and PR-OBS-02 so as to obtain precipitation patterns and retrievals more consistent with each other. This result has been evidenced through a map based analysis of almost coincident overpasses of the AMSU/MHS and SSMIS radiometers and by a quantitative error analysis. This consistency, besides the accuracy of the retrievals, is necessary in order to be able to fully exploit all cross-track and conical scanning radiometer overpasses for a specific event (available at about 3 hour time interval when all DMSP, MetOp, and NOAA satellites are considered), and to be able to use both algorithms for monitoring precipitation at higher spatial/temporal resolution (i.e., exploiting IR observations with blending or morphing techniques as done for PR-OBS-3 and PR-OBS-4), as well as for nowcasting and/or hydrological applications.

4 Product availability

4.1 Terms of Use

All H-SAF products are owned by EUMETSAT, and the EUMETSAT SAF Data Policy applies.

All intellectual property rights of the H-SAF products belong to EUMETSAT. The use of these products is granted to every interested user, free of charge. If you wish to use these products, EUMETSAT's copyright credit must be shown by displaying the words "copyright (year) EUMETSAT" on each of the products used.

4.2 General Information

To access the H-SAF products the user must register at the H-SAF Official Web Portal http://hsaf.meteoam.it/ from which it is possible to access to the "H-SAF Product Download Centre", which allows users to access data as described here following.

1) Access to data produced in the last 60 days must be made by the Official H-SAF FTP server ftp://ftphsaf.meteoam.it (to obtain user and password, please submit registration form on H-SAF Official Web Portal or contact the help desk at us_hsaf@meteoam.it) and via EUMETCAST, a multi-service dissemination system based on standard Digital Video Broadcast (DVB) technology (for more information http://www.eumetsat.int/).
2) The access to the archived data must be performed through an order process. There are two ways to place an order:
    a. the first (link) is a basic function provided directly from the H-SAF Web Portal. It provides all basic functions to carry out orders by selecting one or more products and setting for each selected product an expected time range;
    b. the second function https://eoportal.eumetsat.int/ allows access to EUMETSAT Data Centre. A registration to EUMETSAT portal is required. The EUMETSAT Data Center offers advanced functions of management and control of orders, among which the possibility to make geographical selection of products, to make the cloning of orders, and to monitor the status of the orders.

    In Both cases the orders placed will be submitted for approval and will be delivered within three working days.

Finally, quick-looks of the latest 20 maps can be viewed as PNG images or as an animated slideshow on the H-SAF Web Portal.

4.3 Formats and codes

Three type of files are provided for PR-OBS-1: new rel.:

- the digital data, coded in BUFR;
- the image-like maps, coded in PNG.

In the directory "*utilities*", the folder *Bufr_decode* provides the instructions for reading the digital data. In addition, the output description of PR-OBS-1 is provided in Appendix.

4.4 Description of the files

- Directory: *products*
- Sub-directory: *h01*
- Two folders:
    - h01_cur_mon_buf
    - h01_cur_mon_png

In both directories *products* and *reprocess* the files have identical structures. Next table summarises the situation and provides the information on the file structure, including the legenda.

<table>
<tr><td colspan="2">URL: ftp://ftphsaf.meteoam.it</td><td colspan="3">Credentials: register to hsaf.meteoam.it</td></tr>
<tr><td colspan="5">Directory: products -
Product identifier: h01</td></tr>
<tr><td>h01_cur_mon_buf</td><td rowspan="3" colspan="2">data of current months</td><td>h01_yyyymm_buf</td><td rowspan="3">data of previous months</td></tr>
<tr><td>h01_cur_mon_png</td><td>h01_yyyymm_png</td></tr>
<tr><td></td><td>h01_yyyymm_slm</td></tr>
<tr><td rowspan="3">Files description
(for both directories)</td><td colspan="3">h01_yyyymmdd_hhmm_DMSPss_nnnnn_rom.buf</td><td>digital data</td></tr>
<tr><td colspan="3">h01_yyyymmdd_hhmm_DMSPss_nnnnn_rom2.png</td><td>image data</td></tr>
<tr><td colspan="3">h01_yyyymmdd_hhmm_DMSPss_nnnnn_rom.slm.gz</td><td>surface type</td></tr>
<tr><td>yyyymm:</td><td colspan="4">year, month</td></tr>
<tr><td>yyyymmdd:</td><td colspan="4">year, month, day</td></tr>
<tr><td>hhmm:</td><td colspan="4">hour and minute of first scan line (ascending: southernmost; descending: northernmost)</td></tr>
<tr><td>DMSPss:</td><td colspan="4">name of the satellite (examples: DMSP15 , DMSP16, …)</td></tr>
<tr><td>nnnnn:</td><td colspan="4">orbit number</td></tr>
<tr><td>slm:</td><td colspan="4">map (.txt) recording surface type in 4 steps: 0 = land; 1 = ocean, 2 = coast; 3 = not imaged</td></tr>
</table>

Table 6 Summary instructions for accessing PR-OBS-1 data

Annex 1. PR-OBS-1 new rel. Output description

The PR-OBS1 output is an instantaneous precipitation maps generated from MW images taken by conical scanners on operational satellites in sunsynchronous orbits processed soon after each satellite pass and presented in the natural projection of the image from sunsynchronous orbit. It is encoded as a bufr (edition 4) or, better, as a collection of bufrs where each bufr represents a scan line of the original pass. Its structure (as an example) is the following:

BUFR SECTION 0

LENGTH OF SECTION 0 (BYTES)	8
TOTAL LENGTH OF BUFR MESSAGE (BYTES)	1708
BUFR EDITION NUMBER	4

BUFR SECTION 1

LENGTH OF SECTION 1 (BYTES)	22
BUFR MASTER TABLE	0
ORIGINATING CENTRE	80
ORIGINATING SUB-CENTRE	0
UPDATE SEQUENCE NUMBER	0
FLAG (PRESENCE OF SECTION 2)	0
DATA CATEGORY	12
DATA SUB-CATEGORY	4
LOCAL DATA SUB-CATEGORY	4
VERSION NUMBER OF MASTER TABLE	14
VERSION NUMBER OF LOCAL TABLE	0
YEAR	10
MONTH	1
DAY	1
HOUR	6
MINUTE	20
SECOND	0

It doesn't have section 2.

BUFR SECTION 3

LENGTH OF SECTION 3 (BYTES)	65
RESERVED	0
NUMBER OF DATA SUBSETS	1
FLAG (DATA TYPE/DATA COMPRESSION)	128

And these are the field of section 3 (data section):

	1 SATELLITE IDENTIFIER	0.24800000000000E+003 CODE TABLE 1007
	2 ORBIT NUMBER	0.51965000000000E+005 NUMERIC
	3 YEAR	0.20100000000000E+004 YEAR
	4 MONTH	0.10000000000000E+001 MONTH
	5 DAY	0.10000000000000E+001 DAY
	6 HOUR	0.60000000000000E+001 HOUR
	7 MINUTE	0.20000000000000E+002 MINUTE
HEADER	8 SECOND	0.00000000000000E+000 SECOND
	9 NUMBER OF PIXELS PER COLUMN	0.46600000000000E+003 NUMERIC
	10 NUMBER OF PIXELS PER ROW	0.12800000000000E+003 NUMERIC
	11 SCAN LINE NUMBER	0.10000000000000E+001 NUMERIC
	12 YEAR	0.20100000000000E+004 YEAR
	13 MONTH	0.10000000000000E+001 MONTH
	14 DAY	0.10000000000000E+001 DAY
	15 HOUR	0.60000000000000E+001 HOUR

	16 MINUTE	0.20000000000000E+002 MINUTE
	17 SECOND	0.30000000000000E+002 SECOND
	18 EXTENDED DELAYED DESCRIPTOR REPL	0.12800000000000E+003 NUMERIC
FIELD OF VIEW n°1	19 FIELD OF VIEW NUMBER	0.10000000000000E+001 NUMERIC
	20 LATITUDE (HIGH ACCURACY)	0.70000000000000E+002 DEGREE
	21 LONGITUDE (HIGH ACCURACY)	0.37520000000000E+002 DEGREE
	22 LAND/SEA QUALIFIER	0.10000000000000E+001 CODE TABLE 8012
	23 INTENSITY OF PRECIPITATION (HIGH	0.00000000000000E+000 KG/M**2S
	24 CLOUD PHASE	MISSING CODE TABLE 20056
	25 OBSERVATION QUALITY	0.12000000000000E+002 FLAG TABLE 25053
	26 PER CENT CONFIDENCE	0.00000000000000E+000 %
FIELD OF VIEW n°2	27 FIELD OF VIEW NUMBER	0.20000000000000E+001 NUMERIC
	28 LATITUDE (HIGH ACCURACY)	0.70000000000000E+002 DEGREE
	29 LONGITUDE (HIGH ACCURACY)	0.37190000000000E+002 DEGREE
	30 LAND/SEA QUALIFIER	0.10000000000000E+001 CODE TABLE 8012
	31 INTENSITY OF PRECIPITATION (HIGH	0.00000000000000E+000 KG/M**2S
	32 CLOUD PHASE	MISSING CODE TABLE 20056
	33 OBSERVATION QUALITY	0.12000000000000E+002 FLAG TABLE 25053

These last eight fields are repeated for each field of view.

Annex 2. Introduction to H-SAF

The EUMETSAT Satellite Application Facilities

H-SAF is part of the distributed application ground segment of the "*European Organization for the Exploitation of Meteorological Satellites (EUMETSAT)*". The application ground segment consists of a "*Central Application Facilities*" located at EUMETSAT Headquarters, and a network of eight "*Satellite Application Facilities (SAFs*)", located and managed by EUMETSAT Member States and dedicated to development and operational activities to provide satellite-derived data to support specific user communities (see Figure 11):

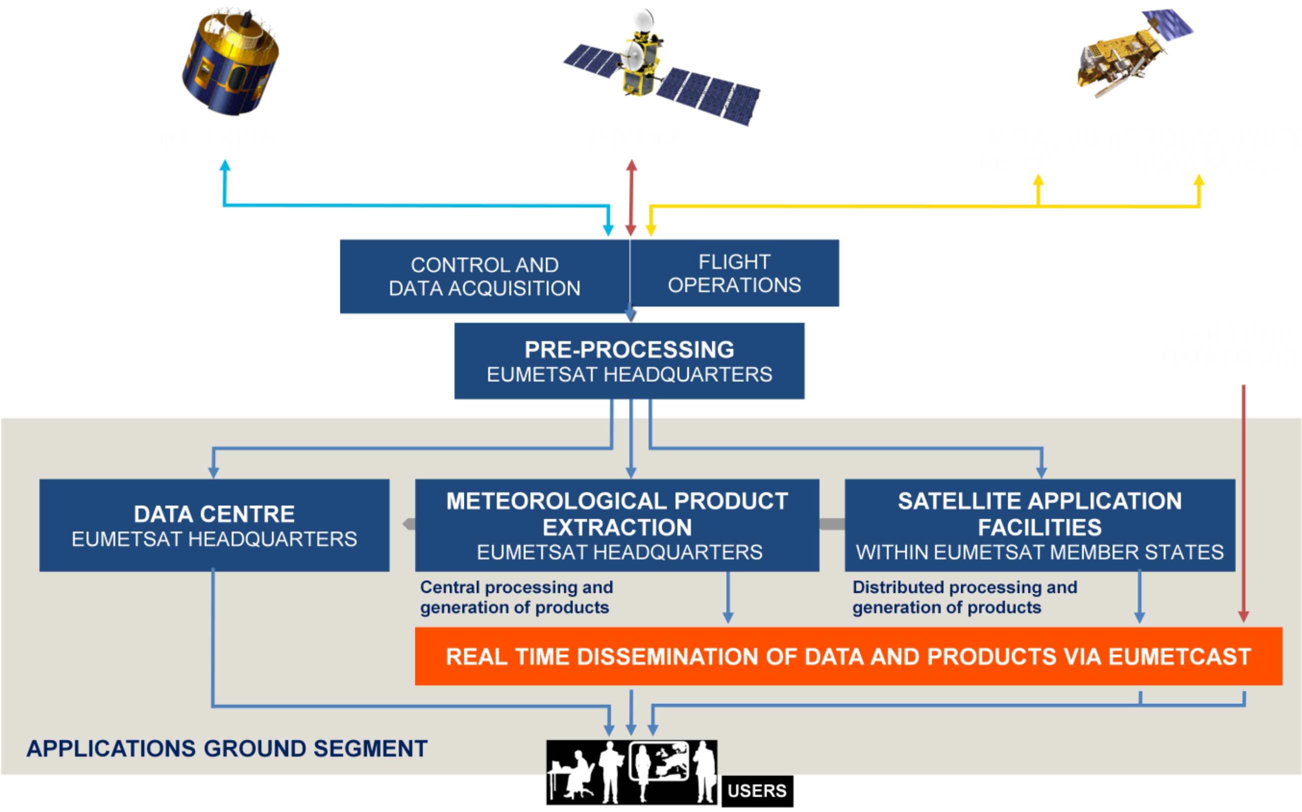

Figure 11: Conceptual scheme of the EUMETSAT Application Ground Segment

Figure 12, here following, depicts the composition of the EUMETSAT SAF network, with the indication of each SAF's specific theme and Leading Entity.

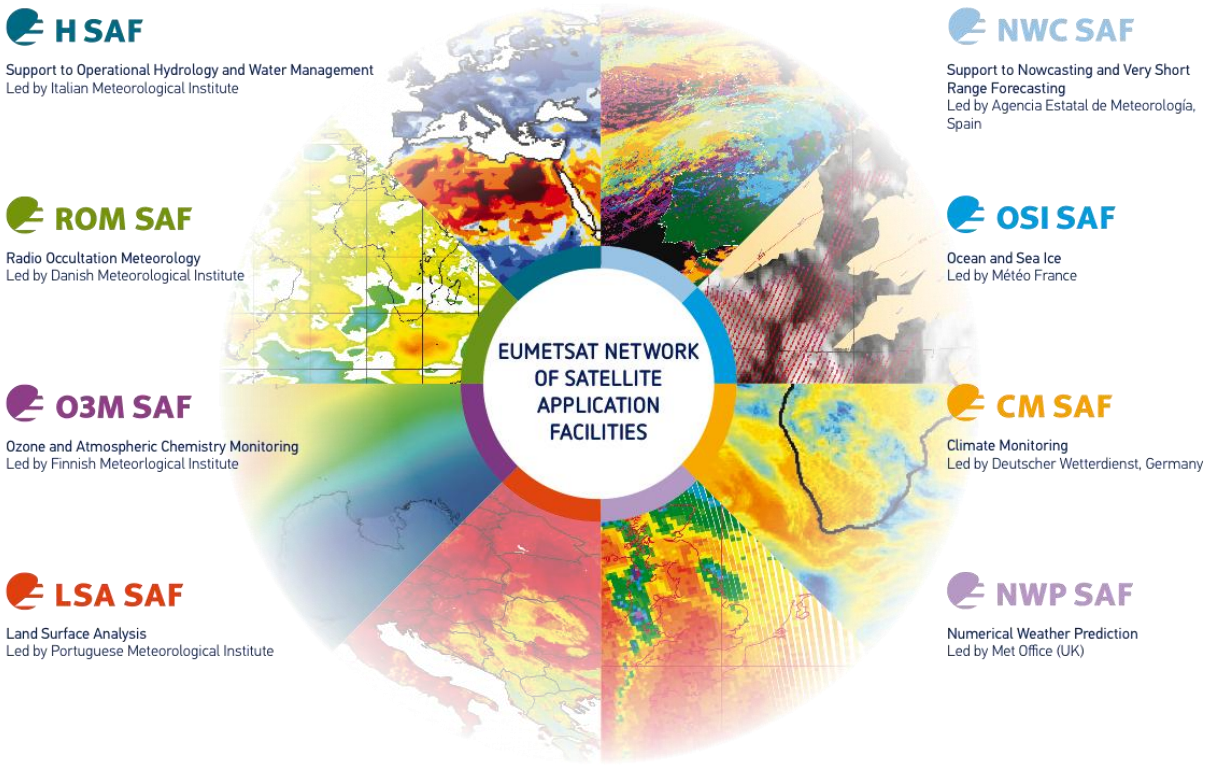

Figure 12: Current composition of the EUMETSAT SAF Network

Purpose of the H-SAF

The main objectives of H-SAF are:

a. ***to provide new satellite-derived products*** from existing and future satellites with sufficient time and space resolution to satisfy the needs of operational hydrology, by generating, centralizing, archiving and disseminating the identified products:
   - precipitation (liquid, solid, rate, accumulated);
   - soil moisture (at large-scale, at local-scale, at surface, in the roots region);
   - snow parameters (detection, cover, melting conditions, water equivalent);

b. ***to perform independent validation of the usefulness of the products*** for fighting against floods, landslides, avalanches, and evaluating water resources; the activity includes:
   - downscaling/upscaling modelling from observed/predicted fields to basin level;
   - fusion of satellite-derived measurements with data from radar and raingauge networks;
   - assimilation of satellite-derived products in hydrological models;
   - assessment of the impact of the new satellite-derived products on hydrological applications.

Products / Deliveries of the H-SAF

For the full list of the Operational products delivered by H-SAF, and for details on their characteristics, please see H-SAF website hsaf.meteoam.it.

All products are available via EUMETSAT data delivery service (EUMETCast, http://www.eumetsat.int/website/home/Data/DataDelivery/EUMETCast/index.html), or via ftp download; they are also published in the H-SAF website hsaf.meteoam.it.

System Overview

H-SAF is lead by the Italian Air Force Meteorological Service (ITAF USAM) and carried on by a consortium of 21 members from 11 countries (see website: hsaf.meteoam.it for details).

Following major areas can be distinguished within the H-SAF system context:

- Product generation area;
- Central Services area (for data archiving, dissemination, catalogue and any other centralized services);
- Validation services area which includes Quality Monitoring/Assessment and Hydrological Impact Validation.

Products generation area is composed of 5 processing centres physically deployed in 5 different countries; these are:

- for precipitation products: ITAF CNMCA (Italy);
- for soil moisture products: ZAMG (Austria), ECMWF (UK);
- for snow products: TSMS (Turkey), FMI (Finland).

Central area provides systems for archiving and dissemination; located at ITAF CNMCA (Italy), it is interfaced with the production area through a front-end, in charge of product collecting.

A central archive is aimed to the maintenance of the H-SAF products; it is also located at ITAF CNMCA.

Validation services provided by H-SAF consists of:

- Hydrovalidation of the products using models (hydrological impact assessment);
- Product validation (Quality Assessment and Monitoring).

Both services are based on country-specific activities such as impact studies (for hydrological study) or product validation and value assessment.

Hydrovalidation service is coordinated by IMWM (Poland), whilst Quality Assessment and Monitoring service is coordinated by DPC (Italy): The Services' activities are performed by experts from the national meteorological and hydrological Institutes of Austria, Belgium, Bulgaria, Finland, France, Germany, Hungary, Italy, Poland, Slovakia, Turkey, and from ECMWF.

Annex 3. Acronyms

AMSU	Advanced Microwave Sounding Unit (on NOAA and MetOp)
AMSU-A	Advanced Microwave Sounding Unit - A (on NOAA and MetOp)
AMSU-B	Advanced Microwave Sounding Unit - B (on NOAA up to 17)
ATDD	Algorithms Theoretical Definition Document
AU	Anadolu University (in Turkey)
BfG	Bundesanstalt für Gewässerkunde (in Germany)
CAF	Central Application Facility (of EUMETSAT)
CDOP	Continuous Development-Operations Phase
CESBIO	Centre d'Etudes Spatiales de la BIOsphere (of CNRS, in France)
CM-SAF	SAF on Climate Monitoring
CNMCA	Centro Nazionale di Meteorologia e Climatologia Aeronautica (in Italy)
CNR	Consiglio Nazionale delle Ricerche (of Italy)
CNRS	Centre Nationale de la Recherche Scientifique (of France)
DMSP	Defense Meteorological Satellite Program
DPC	Dipartimento Protezione Civile (of Italy)
EARS	EUMETSAT Advanced Retransmission Service
ECMWF	European Centre for Medium-range Weather Forecasts
EDC	EUMETSAT Data Centre, previously known as U-MARF
EUM	Short for EUMETSAT
EUMETCast	EUMETSAT’s Broadcast System for Environmental Data
EUMETSAT	European Organisation for the Exploitation of Meteorological Satellites
FMI	Finnish Meteorological Institute
FTP	File Transfer Protocol
GEO	Geostationary Earth Orbit
GRAS-SAF	SAF on GRAS Meteorology
HDF	Hierarchical Data Format
HRV	High Resolution Visible (one SEVIRI channel)
H-SAF	SAF on Support to Operational Hydrology and Water Management
IDL©	Interactive Data Language
IFOV	Instantaneous Field Of View
IMWM	Institute of Meteorology and Water Management (in Poland)
IPF	Institut für Photogrammetrie und Fernerkundung (of TU-Wien, in Austria)
IPWG	International Precipitation Working Group
IR	Infra Red
IRM	Institut Royal Météorologique (of Belgium) (alternative of RMI)
ISAC	Istituto di Scienze dell’Atmosfera e del Clima (of CNR, Italy)
ITU	İstanbul Technical University (in Turkey)
LATMOS	Laboratoire Atmosphères, Milieux, Observations Spatiales (of CNRS, in France)
LEO	Low Earth Orbit
LSA-SAF	SAF on Land Surface Analysis
LST	Local Satellite Time (if referred to time) or Land Surface Temperature (if referred to temperature)
Météo France	National Meteorological Service of France
METU	Middle East Technical University (in Turkey)
MHS	Microwave Humidity Sounder (on NOAA 18 and 19, and on MetOp)
MSG	Meteosat Second Generation (Meteosat 8, 9, 10, 11)
MVIRI	Meteosat Visible and Infra Red Imager (on Meteosat up to 7)
MW	Micro Wave
NEΔT	Net Radiation
NESDIS	National Environmental Satellite, Data and Information Services
NMA	National Meteorological Administration (of Romania)
NOAA	National Oceanic and Atmospheric Administration (Agency and satellite)
NWC-SAF	SAF in support to Nowcasting & Very Short Range Forecasting
NWP	Numerical Weather Prediction
NWP-SAF	SAF on Numerical Weather Prediction

O3M-SAF	SAF on Ozone and Atmospheric Chemistry Monitoring
OMSZ	Hungarian Meteorological Service
ORR	Operations Readiness Review
OSI-SAF	SAF on Ocean and Sea Ice
PDF	Probability Density Function
PEHRPP	Pilot Evaluation of High Resolution Precipitation Products
Pixel	Picture element
PMW	Passive Micro-Wave
PP	Project Plan
PR	Precipitation Radar (on TRMM)
PUM	Product User Manual
PVR	Product Validation Report
RMI	Royal Meteorological Institute (of Belgium) (alternative of IRM)
RR	Rain Rate
RU	Rapid Update
SAF	Satellite Application Facility
SEVIRI	Spinning Enhanced Visible and Infra-Red Imager (on Meteosat from 8 onwards)
SHMÚ	Slovak Hydro-Meteorological Institute
SSM/I	Special Sensor Microwave / Imager (on DMSP up to F-15)
SSMIS	Special Sensor Microwave Imager/Sounder (on DMSP starting with S-16)
SYKE	Suomen ympäristökeskus (Finnish Environment Institute)
T_{BB}	Equivalent Blackbody Temperature (used for IR)
TKK	Teknillinen korkeakoulu (Helsinki University of Technology)
TMI	TRMM Microwave Imager (on TRMM)
TRMM	Tropical Rainfall Measuring Mission UKMO
TSMS	Turkish State Meteorological Service
TU-Wien	Technische Universität Wien (in Austria)
U-MARF	Unified Meteorological Archive and Retrieval Facility
UniFe	University of Ferrara (in Italy)
URD	User Requirements Document
UTC	Universal Coordinated Time
VIS	Visible
ZAMG	Zentralanstalt für Meteorologie und Geodynamik (of Austria)